Colloid Polym Sci 279: 398–403 (2001)

SHORT COMMUNICATION

T. Unruh
H. Bunjes
K. Westesen
M. H. J. Koch

Investigations on the melting behaviour of triglyceride nanoparticles

Received: 27 July 1999
Accepted: 5 October 2000

T. Unruh (✉) · H. Bunjes · K. Westesen
Institut für Pharmazie
Pharmazeutische Technologie
Friedrich-Schiller-Universität Jena
Lessingstrasse 8, 07743 Jena
Germany
e-mail: toun@pt.uni-jena.de
Tel.: +49-3641-949905
Fax: +49-3641-949902

M. H. J. Koch
European Molecular Biology Laboratory
Hamburg Outstation, EMBL c/o DESY
Notkestrasse 85, 22603 Hamburg
Germany

Abstract Suspensions of triglyceride nanoparticles have been proposed as carrier systems for intravenous administration of poorly water soluble drugs. Such nanosuspensions can easily be produced by homogenization of the melted triglyceride in an aqueous phase. Using special emulsifier blends it is possible to obtain suspensions with an average size of the recrystallized particles below 100 nm (photon correlation spectroscopy *z*-average). As can be observed by transmission electron microscopy the particles are very thin platelets with thicknesses in the range of only a few molecular layers. Nanoparticles of saturated monoacid triglycerides (smaller than 200 nm) exhibit uncommon melting behaviour, which is expressed in their differential scanning calorimetry curve by multiple endothermal peaks over a temperature range of about 10 °C. This effect was attributed earlier to the particle thickness distribution in the suspension rather than to polymorphic transitions since all the material exists in the stable β modification. Here we present experimental investigations on the correlation between the melting behaviour of trilaurin nanosuspensions and the particle thickness distribution determined by analysis of difference X-ray diffraction patterns recorded at progressively higher temperatures in the melting range of the particles. Because of the weak X-ray scattering of the systems investigated synchrotron radiation was used besides conventional sources. The Fourier analysis of the difference diffraction patterns is described in detail and the advantages and difficulties in using this method are discussed. It was observed that the melting temperatures of the nanoparticles increase with increasing particle thicknesses. Simultaneously a decrease in the interplanar (001) spacing with increasing particle thickness was found.

Key words Trilaurin · Nanoparticles · Single-line Fourier analysis · Broadening of X-ray reflections · Difference diffraction patterns

Introduction

The formulation of poorly water soluble drugs for intravenous administration is a difficult task in pharmaceutical technology, especially when the drugs are to be targeted to defined tissues. Targeting is strongly desirable for drugs with high toxicity and unspecific action, such as cytostatics, which are often only poorly soluble in water (e.g. taxol). For this purpose aqueous suspensions of triglycerides have been proposed as carrier systems [1]. Owing to the solid state of the carrier particles the release of drugs incorporated into their solid matrix should be slow compared to that from other types of colloidal lipidic carriers such as micelles, emulsions or liposomes.

Colloidally dispersed saturated monoacid triglycerides such as trilaurin exhibit uncommon melting beha-

viour expressed by multiple discrete peaks over a range of about 10 °C in their differential scanning calorimetry (DSC) thermograms (Fig. 1). The melting temperature range of the nanoparticles in Fig. 1 is clearly shifted below the melting temperature of bulk trilaurin at approximately 48 °C [2]. Extensive simultaneous small-angle and wide-angle X-ray diffraction (SWAX) studies on several triglyceride suspensions indicate that the phenomenon is not due to polymorphic transitions, since only the reflections of the β modification are observed upon heating [3], but rather that it is due to particle size effects. The present study was initiated to elucidate the mechanism of the stepwise melting process in more detail by analysis of X-ray Bragg reflection broadening.

Experimental

The investigations were performed on 3 trilaurin nanosuspensions (L1, L2, L3) prepared by high-pressure melt-homogenization at 85 °C. The suspensions consisted of 10% (w/w) trilaurin (approximately 97%, Hüls), Lipoid S100 (Lipoid; 3.2%, 2.4% and 1.6% for L1, L2 and L3, respectively) and water containing 2.25% glycerol and sodium glycocholate (Sigma, approximately 99%; 0.8%, 0.6% and 0.4%, respectively). After preparation of a crude preemulsion by sonification at 85 °C an APV Gaulin Micron Lab 40 homogenizer was used for homogenization. Sample L1 was cycled four times at 1200 bar and once at 1500 bar, L2 was cycled four times at 1000 bar and once at 1300 bar and L3 was cycled four times at 800 bar and once at 1000 bar. The trilaurin droplets were crystallized by cooling the suspension to −9 °C and holding that temperature for 5 min before increasing it again to the storage temperature of about 5 °C.

Photon correlation spectroscopy (PCS) measurements were performed on dilute samples using a ZetaPlus apparatus (Brookhaven Instruments Corporation) and yielded z-averages of the recrystallized particles of 123 nm (L1), 142 nm (L2) and 184 nm (L3).

The DSC measurements were carried out using a Micro DSC III (Setaram) at a scan rate of 0.1 °C/min. The weight of both the sample and the reference (pure water) was about 150 mg.

Preliminary X-ray diffraction measurements were performed with a Kratky camera (Hecus Braun X-ray Systems, Graz) on a conventional X-ray source (Seifert generator ID3003, Cu $K\alpha_{1,2}$, Ni filter). The data presented later were collected on the X33 double focusing synchrotron radiation camera of the EMBL on the storage ring DORIS of the Deutsches Elektronen Synchrotron at Hamburg [4], using a linear delay line readout detector [5]. The data recorded with the line-focused Kratky camera were desmeared using a direct method of beam-height correction [6]. Essentially the same results were obtained in both cases but a much better temperature resolution was achieved with synchrotron radiation, where measuring times are approximately 1000 times shorter. The synchrotron data were recorded at 23, 25, 30, 35, 36, 37, 38–39.5 (0.5 °C steps) and 40–45 °C (0.2 °C steps) for L1, L2 and L3. The sample cells were thermostated with a waterbath (Huber Ministat).

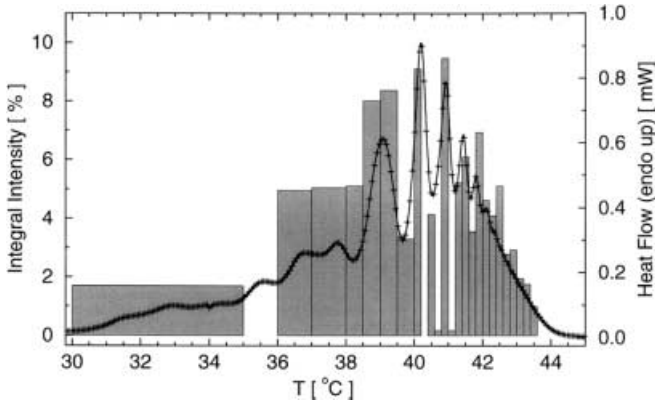

Fig. 1 Differential scanning calorimetry curve of the trilaurin suspension L1 (*right scale*) and histogram of the integrated intensity of the difference diffraction peaks of the L1 sample (*left scale*, see text)

Analysis of difference diffraction patterns

In order to get information on the correlation between the melting temperature and the size of triglyceride nanoparticles the mean domain size of the dispersed nanocrystals was estimated from line broadening of the Bragg reflections at several temperatures in the melting range observed by DSC (Fig. 1). In general it is possible to estimate a particle size distribution from the peak shapes via the second derivative of the size Fourier coefficient A_n^S (n: harmonic number), which is, however, not very accurate because of the sensitivity of differentiation to small experimental errors [7]. This approach also ignores any possible dependence of the lattice constants on the particle size. To overcome these problems for the case of triglyceride nanosuspensions, difference diffraction patterns obtained by subtraction of two patterns recorded at successive temperatures were analysed. In the following this procedure is described in detail, using the example of trilaurin suspension L1.

Single-line method – general procedure

SWAX data of preinvestigations indicated that the trilaurin nanocrystals were in the stable β modification. The layered structure of this modification exhibits a lattice constant, c, of 3.175 nm, which is very large compared to the other lattice constants [2, 8]. Therefore the (00l)-reflections for $l=1$ and $l=2$ occur at low scattering angles well separated from all other reflections, so there is no peak overlap. The scattering intensity of the dispersed nanocrystals is, however, low. Even when using synchrotron radiation the counting statistics deliver difference diffraction patterns of sufficient quality for analysis only for the (001) reflection (scattering angle $2\theta = 2.811°$, $s = \frac{2\sin\theta}{\lambda} = 0.318\,\frac{1}{\mathrm{nm}}$). Thus, the analysis of the difference diffraction data is restricted to a single Bragg reflection and it was performed according to well-established procedures [7, 9, 10].

Standard sample

To get information on the instrumental line broadening the diffraction pattern of trilaurin tempered for 1 week

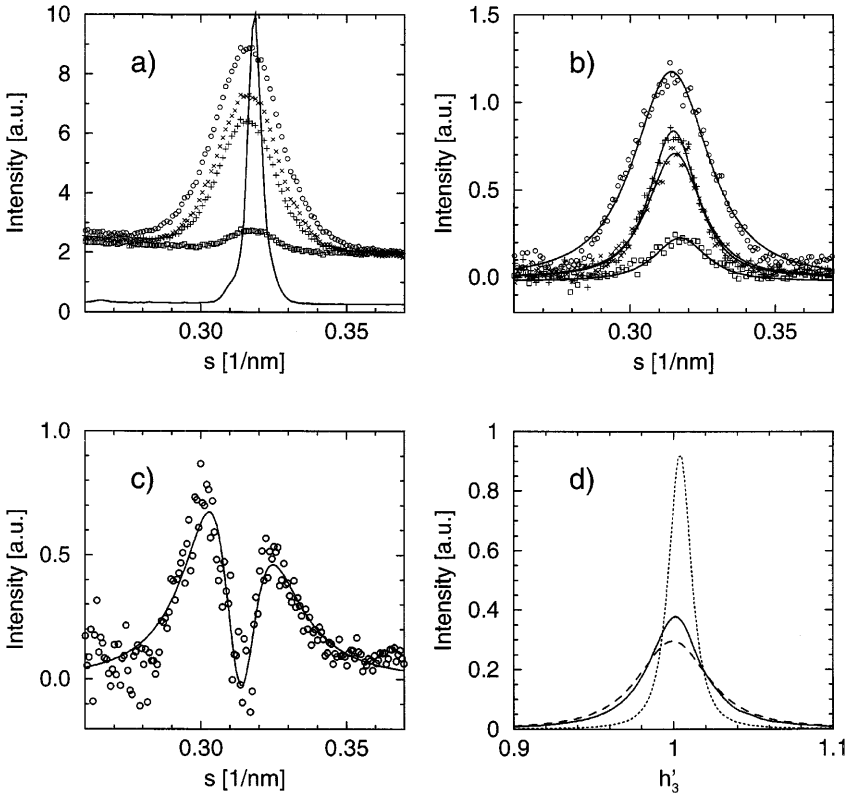

Fig. 2a–d Analysis of the (001) Bragg reflection of sample L1. T_1–T_2 designates the difference diffraction peak calculated by subtraction of the diffraction pattern measured at T_2 (°C) from the pattern measured at T_1 (°C). **a** Data recorded at 39 °C (○), 40 °C (×), 40.8 °C (+) and 43 °C (□). The *solid line* represents the corresponding pattern of the standard sample (see text). **b** Difference diffraction peaks 39.0–39.5 °C (○), 40.0–40.2 °C (×), 40.8–41.0 °C (+) and 43.0–43.2 °C (□). The *solid lines* represent the fits. **c** Difference diffraction peak 36–37 °C and fit (*solid line*). **d** Fits of the (001) reflection of the reference sample (*dotted line*) and of the difference diffraction peak 43.0–43.2 °C (*dashed line*). The *solid line* represents the deconvoluted profile

at 40 °C was recorded at 23 °C (Fig. 2a, reference peak). This measurement was performed with a mixture of 10% trilaurin powder in mannitol. This relatively low concentration guaranteed that the intensities measured were still in the linear range of the detector when using the same camera adjustment as for the nanosuspensions.

General data treatment

The maxima of the (001) and (002) reflections of the standard sample, which could be reproduced before and after the measurement of the nanosuspensions, were used to scale the abscissa (assumed to be linear in s values) of the diffraction patterns. The intensity was corrected for detector response using a pattern produced by a ^{55}Fe source and for the incident intensity detected by an ionization chamber placed in front of the sample.

Correction for the angle dependence of Lorentz and polarization factors

Polarization corrections were neglected as they amount to less than 0.3% in the range of scattering angles ($1.4° < 2\theta < 4.2°$).

Lorentz correction in the small-angle range should be performed after deconvolution [11]; however, when using a Fourier method the particle size/strain analysis is performed in Fourier space and the inverse transformation does not need to be carried out. Therefore, three procedures were tested: no Lorentz correction; Lorentz correction of the standard profile as well as of that of the nanosuspensions; Lorentz correction of the deconvoluted profile and subsequent Fourier transformation. The differences in the domain sizes deduced by these different approaches were smaller than 1%. Lorentz corrections were not applied in subsequent work.

Background determination

One advantage of the analysis of difference diffraction patterns is that the major part of the background, which is quite large and not constant in the 2θ range of interest, is cancelled by the subtraction because the variation of the background within a small temperature range is small.[1] A remaining small background (Fig. 2b) was approximated by a linear function and was also

[1] The change in the small-angle scattering for angles $2\theta < 1°$ is, however, rather large, which may be attributed to the difference of the density of solid and liquid trilaurin.

subtracted. During the subsequent fitting of the difference diffraction peaks a parameter describing an additional constant background was also refined, as described later.

Curve fitting – an effective smoothing procedure

Deconvolution is very sensitive to noise caused, for example, by poor counting statistics. This problem is obviously amplified when analysing difference diffraction patterns rather than the original peaks because the subtraction reduces the signal but not the noise. Therefore, the reference peak and the difference diffraction peaks were approximated by a Pearson VII function each [12] using a Marquardt–Levenberg least-squares fit [13]. The only parameters of the Pearson VII function which were refined are the full width at half maximum parameter, W, the shape parameter, NC, the peak position, $P_{2\theta}$, the maximum intensity, I_0, and a parameter, a, describing a constant background (designation of parameters according to Ref. [12]). The other parameters were set to zero. In the case of SWAX data obtained on a conventional source the Cu Kα_2 correction was performed by fitting a second Pearson VII function simultaneously to the data with the same parameters as the first one but with $I_0(\mathrm{K}\alpha_2) = 0.5 I_0(\mathrm{K}\alpha_1)$ and a peak position relative to $P_{2\theta}$ corresponding to the Cu K$\alpha_{1,2}$ wavelengths $\lambda_1 = 0.15406$ nm and $\lambda_2 = 0.15444$ nm, respectively.

The shape parameter NC = 1.458 deduced from the refinement of the reference peak is also suitable for the difference diffraction peaks. Refining the shape parameter for these peaks leads to a slight improvement in the quality of the fit to the data. This improvement, however, results from a better approximation of the peak basis, whereas the approximation of the central part of the peak is worse. Because of the uncertainties in background correction, the central part of the peak form seems to be more reliable. Therefore, for the refinement of the difference diffraction peaks the shape parameter was kept constant and set to NC = 1.458. A slight additional background correction was consequently allowed by introducing the additive parameter a to the Pearson VII function. This procedure, which gives stable and reasonable fitting results (Fig. 2b), was found to be a very effective method to suppress the "hook" effect [10], indicating that the background subtraction was performed correctly.

The use of split Pearson VII functions does not affect the approximation quality to the data significantly, but the fitting procedure becomes less stable.

After profile fitting, at least 500 values of the line profile were calculated on a h'_3 scale in the range $l'-1/2 < h'_3 < l' + 1/2$ (designation according to Ref. [7]) with

$$h'_3 = \frac{1}{2}\frac{\sin\theta}{\sin\theta_2 - \sin\theta_0} \quad , \tag{1}$$

$$l' = \frac{2a_3}{\lambda_1}\sin\theta_0 \quad , \tag{2}$$

$$a'_3 = \frac{\lambda_1}{4(\sin\theta_2 - \sin\theta_0)} \quad . \tag{3}$$

(2θ: scattering angle, $2\theta_0 = 2.811°$, $2\theta_2 = 4.211°$).

Deconvolution procedure and determination of the mean domain size

The deconvolution with the reference peak was performed in order to eliminate the instrumental broadening from the difference diffraction peaks [14]. The transformations were performed using a fast Fourier transformation algorithm according to Ref. [13]. If necessary the profile data were padded with zeros on both sides to get a number of datapoints which is a power of 2. This discontinuous completion of the data did not affect the quality of the Fourier transform significantly. The Fourier coefficients A_n of the difference diffraction pattern corrected for instrumental broadening were calculated in Fourier space: $A^*_n = H_n/G_n$, with H_n and G_n being the Fourier coefficients of the difference diffraction peak and the reference peak, respectively. The A^*_n values were normalized using the equation $A_n = A^*_n/A^*_0$. An example for deconvolution is given in Fig. 2d.

For the calculation of the mean area-weighted domain size perpendicular to the (001) planes (particle thickness D) it was assumed that the thickness of each particle is constant, whereas a thickness distribution of the particle ensemble is allowed. Sometimes the A_n versus n curves have a small "hook", which means a negative curvature near $n = 0$ [7]. As can be seen in Fig. 3 the A^c_n versus $L = na'_3$ curves for low and medium temperatures do not exhibit any "hook" effect, whereas a very slight "hook" can be observed at high temperatures, which might be due to a small strain in the thicker particles. The values of A^c_n are equal to the A_n values in absence of any "hook" effect. For curves with a "hook" effect the extrapolated tangent at the point with the most negative slope was extrapolated to the y-axis and intersects it at A'_0. For these cases the "hook" effect is corrected according to Ref. [7] using the equation $A^c_n = A_n/A'_0$. Because this effect is extremely small it seems in conjunction with the correction procedure described previously reasonable to determine the particle thickness D directly from the slope $m = \frac{1}{D}$ of the straight part of the A^c_n versus L curves for small n values (Fig. 3).

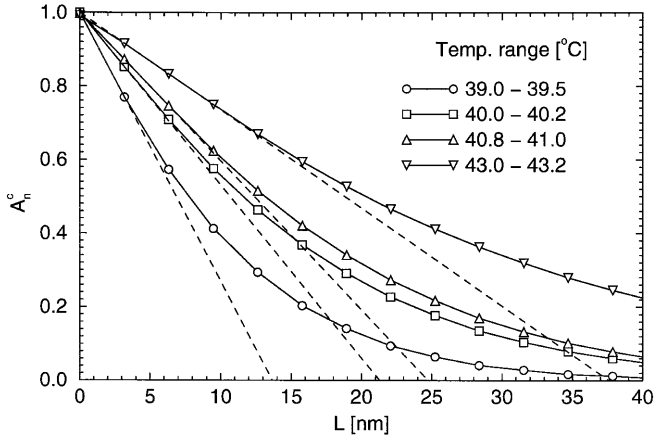

Fig. 3 Corrected Fourier coefficients, A_n^c, versus L of the difference diffraction peaks illustrated in Fig. 2b. The *dashed lines* represent the tangets at the points with the most negative slope. The particle thicknesses, D, can be estimated from the intersections of the tangents with the abscissa (see text)

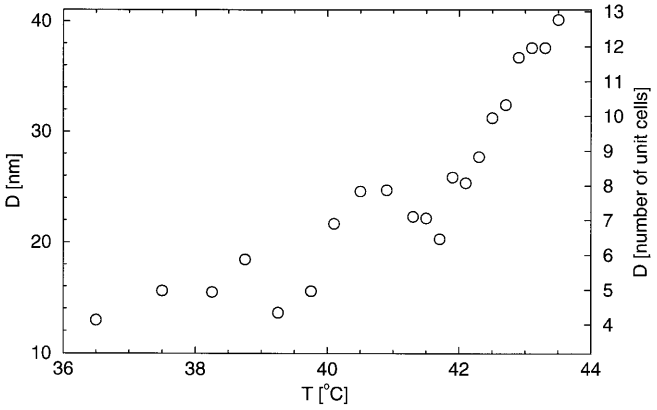

Fig. 4 Correlation of the thickness, D, with the melting temperature, T, of the trilaurin crystals of sample L1. The particle thickness is expressed in nanometres (*left scale*) and in multiples of the unit cell dimension perpendicular to the (001) planes (*right scale*)

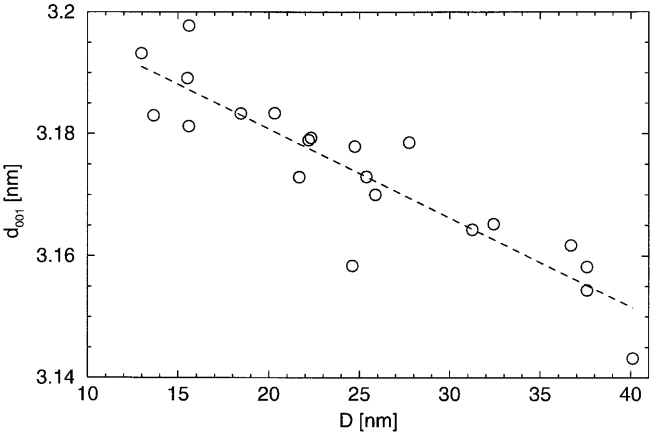

Fig. 5 Dependence of the interplanar (001) spacing, d_{001}, from the particle thickness, D, for sample L1. The *dashed line* represents the linear regression line

Results and discussion

From the analysis of each difference diffraction peak three quantities can be deduced:

1. The integral intensity, which is proportional to the mass of particles melted in the corresponding temperature range.
2. The area-weighted domain size (mean particle thickness) perpendicular to the (001) plane.
3. The mean interplanar spacing, d_{001}, of the melted particles.

The histogram of the integral intensity calculated by numerical integration of the fitted peaks is given in Fig. 1. The values agree well with those of the DSC curve, indicating that the DSC peaks correspond to the loss of crystallinity of the dispersed trilaurin nanoparticles.[2]

This decrease of crystallinity can be attributed to the increase in melting temperature with increasing particle thickness (Fig. 4). However, in contrast to recent investigations on trimyristin nanosuspensions [15, 16], a direct correlation between the particle thickness expressed in number of unit cells along the (001) direction and the peaks in the DSC curve could not be found. This may be explained by the crystallization process as discussed later.

The maxima of the difference diffraction peaks, obtained from the least-squares fits, represent the mean values of the interplanar (001) spacings, d_{001}. The d_{001} values decrease with increasing particle thickness approaching the spacing $d_{001} = 3.140$ nm of bulk trilaurin (Fig. 5). It is remarkable that thin particles are expanded at least in one direction, although the enlarged influence of the interface tension on the thermodynamics of small particles should lead to a contraction of the lattice. Furthermore, it should be remembered that in our experiments the thicknesses of the larger particles were measured at higher temperatures. Thus, when taking into account a thermal expansion of the nanocrystals the true lattice expansion corresponding to the size effect should be even larger than expressed by the data.

Many of the difference diffraction curves for temperatures below 38 °C have a strongly deformed shape as illustrated in Fig. 2c. The observed shape can be interpreted as the result of two simultaneously occurring processes. The first process is the melting of thin

[2] The difference diffraction curves at 35–36 °C and at 40.2–40.4 °C could not be analysed because of peak deformation (see later) and beam interruptions.

particles producing a broad peak in the difference diffraction pattern. The second process is a crystallization of some slightly thicker particles producing a narrower peak with negative amplitude at slightly larger scattering angles in the difference pattern. The solid line in Fig. 2c represents the result of a corresponding least-squares fit of two Pearson VII functions to the data.[3] The increase in the crystallinity of the particles at temperatures just below their melting point may be explained by a temperature-induced acceleration of the segregation process of incorporated phospholipid molecules which are soluble in the liquid triglyceride.

Corresponding slight deformations of the difference diffraction peaks also at higher temperatures cannot be excluded. This might be one reason for the discontinuously increasing D versus T curve, because a small sharp negative peak caused by crystallization can deform the difference diffraction peak in a way that essentially the maximum of the peak produced by the melting is cut. In such a case the difference diffraction peak is apparently broadened. This effect might be responsible for the poor approximation of the fitted curve at the borders of the peak at 39–39.5 °C, leading to an overestimation of the size broadening and consequently to an underestimated particle size (Fig. 4).

Peak deformation is more pronounced for L2 and even more for L3. This effect should be expected because segregation is slower for large particles. In order to overcome this problem we intend to perform further X-ray investigations with synchrotron radiation on samples which have been stored for 1 or 2 years at 23 °C, since for these preliminary X-ray investigations did not show deformations in the difference diffraction peak.

References

1. Westesen K, Siekmann B (1996) Microencapsulation. Dekker, New York, p 213
2. Gibon V, Blanpain P, Norberg B, Durant F (1984) Bull Soc Chim Belg 93:27
3. Bunjes H (1998) Thesis. Jena
4. Koch MHJ, Bordas J (1993) Nucl Instrum Methods 208:461
5. Gabriel A, Dauvergne F (1982) Nucl Instrum Methods 201:223
6. Singh MA, Ghosh SS, Shannon RF Jr (1993) J Appl Crystallogr 26:787
7. Warren BE (1969) X-ray diffraction. Addison-Wesley, Reading, Mass
8. Larsson K (1965) Ark Kemi 23:1
9. Delhez R, de Keijser TH, Mittemeijer EJ (1979) National Bureau of Standards Publication 567. Proceedings of Symposium on Accuracy in Powder Diffraction held at NBS, Gaithersburg, Md, 11–15 June (issued February 1980), pp 213–253
10. Delhez R, de Keijser TH, Mittemeijer EJ (1982) Fresenius Z Anal Chem 312:1
11. Delhez R, Mittemeijer EJ, de Keijser TH, Rozendaal HCF (1977) J Phys E 10:784
12. Young RA (1993) The Rietveld method. Oxford University Press, Oxford
13. Press WH, Teukolsky SA, Vetterling WT, Flannery BP (1995) Numerical recipes in C. Cambridge University Press, Cambridge
14. Stokes AR (1948) Proc Phys Soc Lond 61:382
15. Unruh T, Bunjes H, Westesen K, Koch MHJ (1998) Annual Report. EMBL Hamburg Outstation, p 391
16. Unruh T, Bunjes H, Westesen K, Koch MHJ (1999) J Phys Chem B 103:10373

Note added in proof: The results of recent numerical calculations simulating the X-ray scattering of suspended triglyceride nanoparticles suggest that the observed dependence of the d_{001}-values on the particle thickness, D, are due to the influence of the structure factor of the tripalmitin crystal structure, which strongly changes in the region of the broad (001)-reflection. This means that the d_{001} values calculated from the center of gravity of the (001)-reflections may not reflect the corresponding interplanar distance directly. Further simulations are in progress.

[3] Such a fit is, however, stable only if both peaks are of nearly the same intensity; therefore, the analysis of the difference diffraction curve at 35–36 °C was not possible.